

1  
2  
3  
4  
5  
6  
7  
8  
9  
10  
11  
12  
13  
14  
15  
16  
17  
18  
19  
20  
21

Homologous Expression of Lipid Droplet Protein Enhanced Neutral Lipid  
Accumulation in the Marine Diatom *Phaeodactylum tricornutum*

Kohei Yoneda<sup>1</sup>, Masaki Yoshida<sup>2</sup>, Iwane Suzuki<sup>2</sup>, Makoto M. Watanabe<sup>2</sup>

<sup>1</sup>Graduate School of Life and Environmental Sciences, University of Tsukuba, Ibaraki  
305-8572, Japan

<sup>2</sup>Faculty of Life and Environmental Sciences, University of Tsukuba, Ibaraki 305-8572,  
Japan

Corresponding author: Masaki Yoshida

Faculty of Life and Environmental Sciences, University of Tsukuba, 1-1-1 Tennodai,  
Tsukuba, Ibaraki 305-8572, Japan

Tel.: +81-29-853-4301; Fax: +81-29-853-4301; E-mail:

yoshida.masaki.gb@u.tsukuba.ac.jp

22  
23  
24  
25  
26  
27  
28  
29  
30  
31  
32  
33  
34  
35  
36  
37  
38  
39  
40  
41  
42  
43  
44  
45

## Abstract

Lipid droplets are ubiquitous cellular compartments that store neutral lipids and specific proteins localize on their surface. These proteins work as a scaffold in maintaining the lipid droplet structure or as regulators of lipogenesis or lipolysis. Previously, our group was the first to identify the most abundant lipid droplet protein, namely stramenopile-type lipid droplet protein (StLDP), in the marine diatom *Phaeodactylum tricornutum*; however, its function remains unclear because StLDP does not reveal homology with known lipid droplet proteins and lacks a predictable domain. In this study, we transformed *P. tricornutum* to express a homologous StLDP gene under an *fcpA* promoter in order to determine its function. StLDP expression was strongly enhanced in the mutant (H8), especially in nitrogen-sufficient conditions; however, it was attenuated in nitrogen-deficient conditions. Despite the strong expression, no significant difference was observed in the lipid composition between the wild type (WT) and H8 under nitrogen-sufficient conditions. After cultivation in nitrogen-free medium for 6 days, neutral lipid content significantly increased in H8 than in WT. After 2 days of cultivation in nitrogen-free medium, 97.0% of single cells in WT formed one or two lipid droplets, whereas in H8, this proportion decreased to 78.8%, and the proportion of cells forming three or four lipid droplets increased. Thus, we speculate that StLDP functions to sequester triacylglycerol on the initial lipid droplet formation.

## Keywords

Nitrogen starvation, Overexpression, StLDP, Triacylglycerol

## 46 **Introduction**

47 Microalgal biomass has attracted immense attention as a candidate biodiesel  
48 feedstock due to an increasing interest in the production of renewable feedstock to  
49 protect the global environment and to develop a sustainable society (Huang et al.  
50 2010, Mata et al. 2010). Microalgae can produce several metabolites through  
51 photosynthesis using light energy and carbon dioxide (Mata et al. 2010). The marine  
52 diatom, *Phaeodactylum tricornutum*, is one of the most promising microalgae for  
53 biomass production. It grows faster and can accumulate 20–30% oils (Chisti 2007),  
54 which can be used as a feedstock for biodiesel or dietary supplements containing  
55 polyunsaturated fatty acid, eicosapentaenoic acid (Fajardo et al. 2007). Similar to  
56 other microalgae, the lipid content of *P. tricornutum* increases under nitrogen  
57 deficiency (Abida et al. 2015). Herein, *P. tricornutum* forms oil-rich cellular  
58 compartments called lipid droplets (Guiheneuf et al. 2011). The chief constituent of  
59 lipid droplets in *P. tricornutum* is triacylglycerol (TAG) (Yoneda et al. 2016). Not only  
60 microalgae but also various organisms including mammals, fruits flies, yeast, bacteria,  
61 land plants possess lipid droplets (Murphy and Bance 1999, Murphy 2012); there are  
62 thought to be generated from the phospholipid bilayer of the endoplasmic reticulum  
63 (ER), and certain proteins are found to localize on the droplet surface (Ohsaki et al.  
64 2014). Some of these proteins function as a scaffold for the lipid droplet in  
65 maintaining the globule size, whereas the other proteins reveal diverse functions in  
66 lipid metabolism (lipogenesis and lipolysis), cellular signaling, or membrane trafficking  
67 (Martin and Parton 2006, Pol et al. 2014).

68 Proteomic analyses of fractionated lipid droplets have identified the proteins  
69 present on these lipid droplets in many organisms (Yang et al. 2012). The perilipin  
70 (Plin) and oleosin families of proteins are found as the major proteins on the lipid

71 droplets in mammalian tissues and seed cells of spermatophytes, respectively (Yang  
72 et al. 2012). At present, five proteins belong to the Plin protein family (Plin1–5)  
73 (Kimmel et al. 2010). Plin1 and Plin4 are mainly distributed in the adipose tissue,  
74 Plin2 and Plin3 are ubiquitously expressed in the tissues possessing lipid droplets,  
75 and Plin5 is expressed in the oxidative tissues such as heart muscle (Sztalryd and  
76 Kimmel 2014). Plin1 and Plin2 are the most abundant proteins of cytosolic lipid  
77 droplets in the adipose tissue and the liver, respectively (Sztalryd and Kimmel 2014).  
78 The oleosin family comprises three proteins: oleosin, caleosin, and steroleosin  
79 (Chapman et al. 2012). Oleosin is a major coat protein on the lipid droplets in seed  
80 cells. In the microalgal lipid droplets, homologs of the major lipid droplet protein  
81 (MLDP) were found in the green algae *Chlamydomonas reinhardtii* (Moellering and  
82 Benning 2010, Nguyen et al. 2011), *Dunaliella salina* (Davidi et al. 2012), and  
83 *Lobosphaera incisa* (Siegler et al. 2017) through proteomic analysis, and in  
84 *Scenedesmus quadricauda* using immunology (Javee et al. 2016). In addition,  
85 *Haematococcus* oil globule protein (HOGP), an ortholog of MLDP, was found in the  
86 green algae, *Haematococcus pluvialis* (Peled et al. 2011). Moreover, lipid droplet  
87 proteomics were conducted in the green algae, *Chlorella* sp. (Lin et al. 2012),  
88 endosymbiotic dinoflagellates *Symbiodinium* (Pasaribu et al. 2014), haptophytes  
89 *Tisochrysis lutea* (Shi et al. 2015), eustigmatophytes *Nannochloropsis oceanica*  
90 (Vieler et al. 2012), and the diatom *Fistulifera* sp. JPCC DA0580 (Nojima et al. 2013).  
91 Initially, we performed proteomic analysis on the lipid droplets isolated from *P.*  
92 *tricornutum* and identified a new lipid droplet protein, namely stramenopile-type lipid  
93 droplet protein (StLDP) (Yoneda et al. 2016). Although StLDP was identified as the  
94 main protein of the lipid droplets in *P. tricornutum*, its function remains unclear  
95 because StLDP does not reveal homology with other known lipid droplet proteins and

96 lacks a predictable catalytic domain.

97           According to reports on modifying the expression levels of main lipid droplet  
98 protein, the upregulation of gene expression led to fat accumulation in certain cases.  
99 For example, the adenoviral overexpression of Plin2, a major lipid-droplet-coating  
100 protein in liver, caused hepatosteatosis in mice, and the TAG content increased  
101 two-fold higher in the liver steatosis tissue when compared with the control (Sun et al.  
102 2012). Increasing TAG amounts and dysfunctional effects were also observed with  
103 Plin5 overexpression in the mouse cardiomyocytes (Pollak et al. 2013, Wang et al.  
104 2013). Alternatively, the overexpression of Plin1, a major lipid-droplet-coating protein  
105 in the adipose tissue, led to a leaner phenotype and lower adipose depot weight in  
106 the transgenic mice when compared with the wild type (WT) mice (Miyoshi et al.  
107 2010).

108           In a land plant study, Liu et al. (2013) reported that the transgenic rice seeds  
109 expressing soybean oleosin exhibited around 1.4-fold higher lipid content than WT;  
110 however, the detailed mechanisms facilitating lipid accumulation still remain unclear.  
111 Heterologous expression of Plin and oleosin in the yeast, *Saccharomyces cerevisiae*,  
112 elevated the neutral lipid levels under radiolabeled palmitic acid feeding conditions  
113 (Jacquier et al. 2013). Shemesh et al. (2016) also performed heterologous expression  
114 of the green algal HOGP gene in *P. tricornutum* and reported higher total fatty acid  
115 content and TAG accumulation. To the best of our knowledge, no reports are  
116 available on the homologous expression of the main lipid droplet protein in  
117 microalgae.

118           In this study, we produced a *P. tricornutum* mutant with an enhanced  
119 expression of homologous StLDP gene to determine the function of the lipid droplet  
120 protein, and hypothesized that it would facilitate lipid accumulation.

121

## 122 **Materials and methods**

### 123 **Microalgal strain and culture conditions**

124 *P. tricornutum* CCAP1052/6 was cultivated at 20 °C with continuous light at 70  $\mu\text{mol}$   
125  $\text{photons m}^{-2} \text{s}^{-1}$ . Half strength seawater, prepared using 17  $\text{gL}^{-1}$  of Coral Pro salt (Red  
126 Sea, Eilat, Israel) and enriched with f/2 nutrient (Guillard and Ryther 1962), was used  
127 for the strain maintenance and during the course of transformation. 4f medium  
128 containing 8-fold higher nitrate and phosphate concentrations than in f/2 was used in  
129 the main cultivation experiment. We performed the main cultivation in 200 mL  
130 Erlenmeyer flasks with 120 mL liquid medium, and ambient air was bubbled for  
131 agitation.

132

### 133 **Construction of plasmids**

134 For the expression of StLDP-enhanced green fluorescent protein (EGFP) fusion  
135 protein and histidine-tagged (his-tag) StLDP in *P. tricornutum*, we constructed two  
136 plasmids: pPT-FP and pPT-StLDP-his. The pPT-FP plasmid contained the expression  
137 cassette of the fusion gene comprising EGFP gene fused to the C-terminal of the  
138 StLDP gene from *P. tricornutum*. We deleted the stop codon from StLDP and the start  
139 codon from EGFP and connected them with glycine linker ( $\times 5$  glycine). The  
140 pPT-StLDP-his plasmid comprised StLDP gene with six additional histidines at the  
141 C-terminal.

142 The pPha-T1 plasmid reported by Zaslavskaia et al. (2000) was used as the  
143 backbone of both expression plasmids. The multicloning site (MCS) of the pPha-T1  
144 was located between the fucoxanthin–chlorophyll binding protein (fcp) A promoter  
145 and terminator. Thus, the inserted gene in the MCS was expressed under the control

146 of the *fcpA* promoter. In addition, pPha-T1 contained a *sh ble* gene expression  
147 cassette to confer zeosin resistance. The pPha-T1 and pPTEGfp plasmids  
148 comprising the EGFP gene in the pPha-T1 plasmid (Zaslavskaia et al. 2000) were a  
149 kind gift from Prof. Peter Kroth, University of Konstanz. The primers used in this study  
150 are summarized in Table S1.

151 For the constructing pPT-FP, DNA fragments of StLDP and EGFP were  
152 individually amplified from the genomic DNA of *P. tricornutum* and pPTEGfp by  
153 polymerase chain reaction (PCR) using the primer sets LD\_F/FP-LD\_R and  
154 FP-EGFP\_F/EGFP\_R, respectively. Both fragments were then mixed and fused using  
155 PCR. The fused PCR product was double-digested by EcoRI and HindIII, and was  
156 inserted into the corresponding cloning site in the pPha-T1 with DNA Ligation Kit,  
157 Mighty Mix (Takara Bio, Otsu, Japan).

158 For constructing pPT-StLDP-his, DNA fragment of StLDP was amplified from  
159 genomic DNA by PCR using a LD\_F/LD-His\_R primer set. The PCR product was then  
160 inserted into the EcoRI/HindIII sites in the pPha-T1 plasmid in similar manner.

161 Eventually, we confirmed the DNA sequences of the inserted genes in the  
162 plasmids by DNA sequencing using a BigDye Cycle Sequencing Kit (Thermo Fisher  
163 Scientific, Boston, MA, USA) and a 3130 Genetic Analyzer (Applied Biosystems,  
164 Carlsbad, CA, USA).

165

## 166 **Transformation of diatoms**

167 The diatom cells were transformed using the protocol described by Zaslavskaia et al.  
168 (2000) with minor modifications. Approximately  $7 \times 10^7$  cells were spread on an agar  
169 plate and bombarded using a BioRad Biolistic PDS-1000/He Particle Delivery System  
170 (BioRad, Hercules, CA, USA) with a 1350 psi rupture disc. Gold particles (1.0  $\mu\text{m}$

171 diameter) that coated with 3  $\mu\text{g}$  of circular plasmid DNA, 0.1 M spermidine, and 2.5 M  
172  $\text{CaCl}_2$  were bombarded twice per plate. After an overnight recovery culture, the  
173 bombarded diatom cells were then cultivated on a selection plate containing 50  $\mu\text{g}$   
174  $\text{mL}^{-1}$  zeocin. Gene integration into the genomic DNA was confirmed by PCR using the  
175 specific primers for the his-tag StLDP (LD\_F/6His-spe\_R) and StLDP-EGFP  
176 (LD\_F/EGFP\_R).

177

### 178 **Microscopic observation of the localization of the StLDP-EGFP fusion protein**

179 We cultivated the mutants in f/2 medium under static conditions as described  
180 elsewhere and microscopic images were captured using an Olympus BX53  
181 microscope system (Olympus, Center Valley, PA, USA) equipped with a BNA  
182 fluorescent mirror (green filter; excitation, 475–495 nm, absorption, 510–550 nm).

183

### 184 **Cultivation experiment in nitrogen-deficient medium**

185 WT and his-tagged StLDP-expressing strains (His1-22-8; H8) were precultured in 4f  
186 medium for 1 week and were inoculated in fresh 4f medium. The initial cell  
187 concentrations were adjusted to 0.15 at an optical density of 750 nm. The strains  
188 were cultivated in nitrogen-sufficient medium for 4 days, and were then transferred to  
189 nitrogen-deficient 4f medium that lacked a nitrogen source. Before the transfer, we  
190 washed the cells twice with nitrogen-deficient medium. Cultivation under  
191 nitrogen-deficient conditions lasted for 6 days.

192

### 193 **Dry cell weight (DCW) measurement and lipid analysis**

194 For DCW measurements, cells in 10 mL culture broth were harvested on the  
195 preweighted GF/C glass filter, and were dried at 55  $^{\circ}\text{C}$  in an oven. The dried biomass



196 residues on the filter were then gravimetrically measured.

197 We extracted crude lipids using Folch method (Folch et al. 1957). The wet  
198 biomass pellet obtained by centrifugation of 50 mL of culture broth was used directly  
199 for chloroform/methanol extraction. The amount of the crude lipid extracts was  
200 measured gravimetrically after the extraction. The composition of neutral and polar  
201 lipids was determined using silica gel column chromatography with Silica Gel 60  
202 (Merck, Darmstadt, Germany) as a support. The crude lipids were eluted first using  
203 chloroform (four times the volume of the column bed), followed by the same volume  
204 of methanol. The chloroform fraction contained neutral lipids, mainly TAG, whereas  
205 the methanol fraction contained polar lipids such as phospholipids and glycolipids.

206

#### 207 **RNA extraction and qRT-PCR**

208 The RNA extraction procedure and qRT-PCR for the quantification of StLDP  
209 expression were performed as per our previous report (Yoneda et al. 2016). In this  
210 study, we used TRIzol reagent (Thermo Fisher Scientific, Boston, MA, USA) and  
211 RNeasy Mini Kit (Qiagen, Hilden, Germany) for total RNA extraction. A PrimeScript  
212 RT Reagent Kit with gDNA Eraser (Takara Bio, Shiga, Japan) was used to eliminate  
213 residual genomic DNA and cDNA synthesis, and SYBR Premix ExTaq II (Tli RNaseH  
214 Plus) (Takara Bio, Shiga, Japan) was used for the two-step real-time qRT-PCR.

215

#### 216 **Quantification of lipid droplet size and number**

217 Lipid droplet were stained with Nile red (Wako, Osaka, Japan) and were observed  
218 under fluorescent microscopy. The captured images were analyzed using ImageJ  
219 (Abramoff et al. 2004). The dots derived from the Nile red-stained lipid droplets were  
220 numbered and the size of each fluorescent area was measured using the ImageJ.

221 The diameters of the lipid droplets were calculated from the area, and the numbers of  
222 lipid droplets per cell were manually enumerated from the processed images.

223

## 224 **Results**

### 225 **Localization of StLDP–EGFP fusion protein**

226 We previously identified StLDP from the lipid droplet fraction obtained from *P.*  
227 *tricornutum* (Yoneda et al. 2016); however, we did not confirm the localization of  
228 StLDP. Therefore, we attempted to express the StLDP–EGFP fusion protein in *P.*  
229 *tricornutum*. Figure 1 presents the subcellular localization of EGFP and the  
230 StLDP–EGFP fusion protein. EGFP fluorescence was broadly observed in the cell  
231 (Fig. 1A), whereas the green fluorescence from the fusion protein (StLDP–EGFP)  
232 was localized at the lipid droplet in *P. tricornutum* (Fig. 1B). Thus, StLDP was  
233 confirmed as a lipid droplet protein in *P. tricornutum*.

234

### 235 **Growth curve, DCW, lipid content, and expression levels of StLDP in WT and** 236 **mutant**

237 To determine the function of StLDP, WT and his-tagged StLDP-expressing strain (H8)  
238 were cultivated in nitrogen-sufficient medium for 4 days and in nitrogen-deficient  
239 medium for 6 days. Figure 2A presents the growth curve of these strains and Figure  
240 2B reveals the DCW and lipid amounts at the end of cultivation (Day 10). No  
241 significant differences were seen in the growth, DCW, or crude lipid amounts between  
242 the strains. Figure 2C represents the expression levels of StLDP at Days 4, 7, and 10.  
243 StLDP expression in H8 was 57-fold higher than that in WT at Day 4; however, the  
244 enhanced StLDP expression in H8 decreased at Day 7 to a level that was 1.2-fold  
245 higher than the WT, and finally reached the same level as the WT at Day 10. Gene

246 expression of the introduced his-tagged StLDP under the control of fcpA promoter  
247 was attenuated after the prolonged cultivation period under nitrogen starvation.

248

#### 249 **Lipid composition in WT and mutant**

250 Figure 3 indicates the proportion of neutral and polar lipids in WT and H8 mutant at  
251 Days 4 and 10. The composition of neutral lipids in the crude lipid was similar in both  
252 strains at Day 4 ( $33.2 \pm 1.3\%$  and  $33.4 \pm 1.4\%$  in WT and H8, respectively; Fig. 3A). A  
253 significant increase in the percentage composition of neutral lipid was observed at  
254 Day 10 ( $45.3 \pm 2.8\%$  and  $53.5 \pm 2.3\%$  in WT and H8, respectively; Fig. 3B;  $P = 0.007$ ,  
255 Student's t-test,  $n = 3$ ). On the contrary, the percentage composition of the polar  
256 lipids significantly decreased in the H8 mutant when compared with WT (Fig. 3B;  $P =$   
257  $0.035$ , Student's t-test,  $n = 3$ ). When we converted the crude lipids to DCW, a  
258 significant increase in the neutral lipid content was observed in the H8 mutant (Fig.  
259 3C;  $P = 0.026$ , Student's t-test,  $n = 3$ ). This suggested that the homologous  
260 expression of StLDP promoted the accumulation of neutral lipid.

261

#### 262 **Microscopic observation during cultivation in nitrogen-deficient medium**

263 Figure 4 presents the microscopic images of WT and H8 mutant at Days 4, 6, and 10.  
264 At Day 4, just before inoculation into the nitrogen-deficient medium, none of strains  
265 formed lipid droplets in the cells (Fig. 4A). This observation revealed that the  
266 overexpression of StLDP per se did not trigger the formation of lipid droplets. Even at  
267 Day 5, scanty lipid droplets were seen; however, after Day 6, the lipid droplets were  
268 observed in WT and H8 mutant (Fig. 4B), revealing that the timing of induction of lipid  
269 droplet formation was same in both strains. At the end of cultivation (Day 10), we  
270 could observe larger lipid droplets in H8 than WT (Fig. 4C), suggesting that lipid

271 droplet fused with each other as the result of attenuation of StLDP expression in the  
272 H8 strain under prolonged cultivation period under nitrogen starvation.

273

#### 274 **Lipid droplet diameter and the number of lipid droplets per cell**

275 As shown in Figure 3 (B, C), the neutral lipid composition increased in the H8 mutant  
276 at the final day (Day 10). The expression level of StLDP was strongly enhanced in the  
277 H8 mutant at Day 4, prior to cultivation in the nitrogen-deficient medium (Fig. 2C);  
278 however, neutral lipid accumulation and lipid droplet formation was not observed at  
279 the Day 4 (Figs. 3A and 4A). Thus, the major effects of the StLDP expression  
280 occurred after reinoculation into the nitrogen-deficient medium. We speculated that  
281 the major effect was occurred at the initial stage of nitrogen deprivation because the  
282 expression of introduced his-tagged StLDP decreased to the same level as the WT at  
283 later stages (Day 10, Fig. 2C). Herein, we focused on the size and number of lipid  
284 droplets, especially at Day 6, the initial stage of lipid droplet formation.

285 Figure 5 (A, B) presents the distribution of the diameter of each lipid droplet at  
286 Days 6 and 10. At Day 6, the distribution of the lipid droplet diameter was similar in  
287 the WT and H8 mutant (Fig. 5A), and the average diameter did not differ either of the  
288 strains ( $1.26 \pm 0.47 \mu\text{m}$  and  $1.36 \pm 0.52 \mu\text{m}$  in WT and H8, respectively). Alternatively,  
289 the proportion of larger lipid droplet increased in H8 mutant at Day 10 (Fig. 5B) and  
290 reflected higher neutral lipid content in H8 mutant at Day 10 (Fig. 3B). Figure 5C  
291 reveals the number of lipid droplets per cell at Day 6. In WT, almost all single cells  
292 (97.0%) formed one or two lipid droplet(s), whereas in the H8 mutant, the proportion  
293 decreased to 78.8% and the proportion of the cells that formed three or four lipid  
294 droplets was increased (15.1 and 6.0%, respectively; Fig. 5C). In particular, on the  
295 size distribution, the lipid droplets were similar; however, the number of lipid droplets

296 per cell changed between the strains at Day 6. These observation suggested that the  
297 enhanced StLDP expression increased the number of lipid droplets per cell at the  
298 initial nitrogen-deficient period and led to the promotion of the neutral lipid  
299 accumulation.

300

## 301 **Discussion**

### 302 **Growth and expression levels of StLDP in mutant**

303 As shown in Figure 2A, the expression of his-tagged StLDP in the H8 mutant did not  
304 lead to growth inhibition; however, overexpression of StLDP in the H8 mutant was  
305 restricted on Day 4 (Fig. 2C). This was explained by the attenuation of expression by  
306 the *fcpA* promoter under nitrogen deficiency. A transcriptomic study of *P. tricornutum*  
307 demonstrated that the LHCF1 gene (also known as *fcpA*) and several genes related  
308 to the photosynthesis and pigment biosynthesis were repressed during nitrogen  
309 deprivation (Alipanah et al. 2015). To improve the expression levels under nitrogen  
310 deprivation, Shemesh et al. (2016) developed a new promoter of the DGAT1 gene in  
311 *P. tricornutum*; however, they reported that although pDGAT1 promoted gene  
312 expression under nitrogen deprivation, the expression levels were still lower than the  
313 other promoters (e.g., *fcpA*). Utilization of pDGAT1 or other promoters that express  
314 under nitrogen deprivation requires for further investigation.

315

### 316 **Accumulation of neutral lipids in nitrogen-deficient conditions and function of** 317 **StLDP**

318 Despite the restriction of overexpression by the *fcpA* promoter, significant differences  
319 were observed in the lipid composition (Fig. 3). In this study, the percentage neutral  
320 lipid content was increased by 18% in the H8 mutant when compared with WT (Fig.

321 3B). Elevation of neutral lipid due to the expression of lipid droplet proteins has often  
322 been reported in previous studies (Sun et al. 2012, Pollak et al. 2013, Wang et al.  
323 2013). Lipid droplet-coating proteins likely function to protect stored lipid (i.e., TAG)  
324 from cytosolic lipases. Thus, one of the reasons for oil accumulation induced by  
325 StLDP overexpression could be due to the enhanced protection ability and the  
326 interruption of hydrolyzes by the lipases (Miyoshi et al. 2010, Pollak et al. 2013).

327 In transgenic mice, the overexpression of Plin1 led to a leaner phenotype and  
328 lower fat accumulation in the adipocytes. This was explained by the differentiation of  
329 white adipose tissue to a more energy-consuming brown adipose-like tissue that led  
330 to higher energy expenditure, upregulation of mitochondrial fatty acid  $\beta$ -oxidation, and  
331 downregulation of lipogenic genes (Sawada et al. 2010, Miyoshi et al. 2010).  
332 Alternatively, the overexpression of Plin5 in mouse heart tissue slightly  
333 downregulated the mitochondrial medium chain acyl-CoA dehydrogenase that is  
334 related to fatty acid  $\beta$ -oxidation (Wang et al. 2013). It is likely that StLDP linked to the  
335 lipogenic or lipolytic pathways especially under nitrogen deficiency. Alternatively, it is  
336 not likely in nitrogen-sufficient conditions because the lipid composition in the H8  
337 mutant did not differ from WT in the nitrogen-sufficient conditions (Fig. 3A).

338 According to Jacquier et al. (2013), heterologous expression of Plin family  
339 proteins and oleosin in the yeast, *S. cerevisiae*, led to increased TAG levels. Deletion  
340 mutants of phosphatidate phosphatase, PAH1, which catalyzes the  
341 dephosphorylation of phosphatidate during the glycerolipid biosynthesis, could not  
342 form lipid droplets in the cell, and TAG and sterol ester (STE) existed at the bilayer of  
343 ER membrane in the *pah1* $\Delta$  yeast mutant (Jacquier et al. 2013). Irregular  
344 accumulation of neutral lipids on the ER membrane is unfavorable for ER-localizing  
345 lipogenic enzymes as it changes the physical properties of the ER membrane and the

346 products remain at the reaction site. The expression of Plins and oleosin in the *pah1Δ*  
347 mutant led to the relocation of these neutral lipids into the lipid droplet and the  
348 enhanced TAG and STE biosynthesis (Jacquier et al. 2013). The authors concluded  
349 that the accumulated neutral lipids on the ER membrane were released by the  
350 expression of Plin and oleosin that facilitated the sequestration of synthesized neutral  
351 lipid product (i.e., TAG and STE) from the ER to the lipid droplet. In our study, after  
352 cultivation in the nitrogen-deficient medium, the percentage composition of neutral  
353 lipid was increased in the H8 mutant (Fig. 3C), and the proportion of cells that had  
354 more than three lipid droplets in a single cell at Day 6 was increased in the H8 mutant  
355 (Fig. 5C). Thus, we hypothesized that StLDP facilitated the sequestration of TAG at  
356 the initial stage of lipid droplet formation and led to an increase in the number of lipid  
357 droplets in the H8 mutant. At the end of the cultivation (Day 10), the proportion of  
358 large lipid droplets increased in the H8 mutant (Fig. 5B). We speculated that tiny lipid  
359 droplets generated at Day 6 fused with each other due to a decrease in coating  
360 protein caused by the attenuation of StLDP expression during nitrogen deficiency (Fig.  
361 2C), producing large lipid droplets observed at Day 10 in the H8 mutant. Prolonged  
362 upregulation of the StLDP gene in the nitrogen-deficient culture may enhance further  
363 lipid accumulation through the physical barrier effects of lipid-droplet-coating proteins.  
364 Further studies are necessary to determine whether StLDP is involved in the  
365 regulation of lipogenic or lipolytic enzymes in the nitrogen-deficient conditions.

366

367

### 368 **Acknowledgments**

369 This study was supported by the Grant-in-Aid for Japan Society for the Promotion of  
370 Science (JSPS) Research Fellow [JSPS KAKENHI Grant Number JP17J03747 to

371 K.Y.].

372

373

374 **Compliance with Ethical Standards**

375 The authors declare no conflicts of interest.

376

377

378



379 **References**

380 Abida H, Dolch LJ, Meï C, Villanova V, Conte M, Block MA, Finazzi G, Bastien O,  
381 Tirichine L, Bowler C, Rébeillé F (2015) Membrane glycerolipid remodeling triggered  
382 by nitrogen and phosphorus starvation in *Phaeodactylum tricornutum*. *Plant Physiol*  
383 167: 118-136.

384

385 Abramoff MD, Magalhaes PJ, Ram SJ (2004) Image processing with Image. J  
386 *Biophotonical International* 11: 36-42.

387

388 Alipanah L, Rohloff J, Winge P, Bones AM, Brembu T (2015) Whole-cell response to  
389 nitrogen deprivation in the diatom *Phaeodactylum tricornutum*. *J. Exp Bot* 66:  
390 6281-6296.

391

392 Chapman KD, Dyer JM, Mullen RT (2012) Biogenesis and functions of lipid droplets  
393 in plants. *J Lipid Res* 53: 215-216.

394

395 Chisti Y (2007) Biodiesel from microalgae. *Biotechnol Adv* 25: 294-306.

396

397 Davidi L, Katz A, Pick U (2012) Characterization of major lipid droplet proteins from  
398 *Dunaliella*. *Planta* 236: 19-33.

399

400 Fajardo AR, Cerdan LE, Medina AR, Fermamdez FGA, Moreno PAG, Grima EM  
401 (2007) Lipid extraction from the microalga *Phaeodactylum tricornutum*. *Eur J Lipid Sci*  
402 *Technol* 109: 120-126.

403

404 Folch J, Lee M, Stanley GHS (1957) A simple method for the isolation and purification  
405 of total lipids from animal tissues. J Biol Chem 226: 497-509.  
406

407 Guiheneuf F, Leu S, Zarka A, Khozin-Goldberg I, Khalilov I, Boussiba S (2011) Cloning  
408 and molecular characterization of a novel acyl-CoA: diacylglycerol acyltransferase  
409 1-like gene (PtDGAT1) from the diatom *Phaeodactylum tricornutum*. FEBS J 278:  
410 3651-3666.  
411

412 Guillard RRL, Ryther JH (1962) Studies of marine planktonic diatoms. I. *Cyclotella*  
413 *nana* Hustedt and *Detonula confervaceae* (Cleve) Gran. Can J Microbiol 8: 229-239  
414

415 Huang G, Chen F, Wei D, Zhang X, Chen G (2010) Biodiesel production by microalgal  
416 biotechnology. Appl Energ 87: 38-46.  
417

418 Jacquier N, Mishra S, Choudhary V, Schneiter R (2013) Expression of oleosin and  
419 perilipins in yeast promotes formation of lipid droplets from the endoplasmic reticulum.  
420 J Cell Sci 126: 5198-5209.  
421

422 Javee A, Sulochana SB, Pallisery SJ, Arumugam M (2016) Major lipid body protein:  
423 A conserved structural component of lipid body accumulated during abiotic stress in *S.*  
424 *quadricauda* CASA-CC302. Front Energ Res 4: 37.  
425

426 Kimmel AR, Brasaemle DL, McAndrews-Hill M, Sztalryd C, Londos C (2009) Adoption  
427 of PERILIPIN as a unifying nomenclature for the mammalian PAT-family of  
428 intracellular lipid storage droplet proteins. J Lipid Res 51: 468-471.

429

430 Lin I, Jiang P, Chen C, Tzen JTC (2012) A unique caleosin serving as the major  
431 integral protein in oil bodies isolated from *Chlorella* sp. cells cultured with limited  
432 nitrogen. *Plant Physiol Biochem* 61:80-87.

433

434 Liu WX, Liu HL, Qu LQ (2013) Embryo-specific expression of soybean oleosin altered  
435 oil body morphogenesis and increased lipid content in transgenic rice seeds. *Theor*  
436 *Appl Genet* 126: 2289-2297.

437

438 Martin S, Parton RG (2006) Lipid droplets: a unified view of a dynamic organelle. *Nat*  
439 *Rev Mol Cell Bio* 7: 373-378.

440

441 Mata TM, Martins AA, Caetano NS (2010) Microalgae for biodiesel production and  
442 other applications: A review. *Renew Sust Energ Rev* 14: 217-232.

443

444 Miyoshi H, Souza SC, Endo M, Sawada T, Perfield JW, Shimizu C, Stancheva Z,  
445 Nagai S, Strissel KJ, Yoshioka N, Obin MS (2010) Perilipin overexpression in mice  
446 protects against diet-induced obesity. *J Lipid Res* 51: 975-982.

447

448 Moellering ER, Benning C (2010) RNA interference silencing of a major lipid droplet  
449 protein affects lipid droplet size in *Chlamydomonas reinhardtii*. *Eukaryot Cell* 9:  
450 97-106.

451

452 Murphy DJ, Vance J (1999) Mechanisms of lipid-body formation. *Trends Biochem Sci*  
453 24: 109-115.

454

455 Murphy DJ (2012) The dynamic roles of intracellular lipid droplets: from archaea to  
456 mammals. *Protoplasma* 249: 541-585.

457

458 Nguyen HM, Baudet M, Cuine S, Adriano JM, Barthe D, Billon E, Bruley C, Beisson F,  
459 Peltier G, Ferro M, Li-Beisson Y (2011) Proteomic profiling of oil bodies isolated from  
460 the unicellular green microalga *Chlamydomonas reinhardtii*: With focus on proteins  
461 involved in lipid metabolism. *Proteomics* 11: 4266-4273.

462

463 Nojima D, Yoshino T, Maeda Y, Tanaka M, Nemoto M, Tanaka T (2013) Proteomics  
464 analysis of oil body associated proteins in the oleaginous diatom. *J Proteome Res* 12:  
465 5293-5301.

466

467 Ohsaki Y, Suzuki M, Fujimoto T (2014) Open questions in lipid droplet biology. *Chem*  
468 *Biol* 21: 86-96.

469

470 Pasaribu B, Lin IP, Tzen JT, Jauh GY, Fan TY, Ju YM, Cheng JO, Chen CS, Jiang PL  
471 (2014) SLDP: a novel protein related to caleosin is associated with the endosymbiotic  
472 *Symbiodinium* lipid droplets from *Euphyllia glabrescens*. *Mar Biotechnol* 16: 560-571.

473

474 Peled E, Leu S, Zarka A, Weiss M, Pick U, Khozin-Goldberg I, Boussiba S (2011)  
475 Isolation of a novel oil globule protein from the green alga *Haematococcus pluvialis*  
476 (Chlorophyceae). *Lipids* 46: 851-861.

477

478 Pol A, Gross SP, Parton RG (2014) Biogenesis of the multifunctional lipid droplet:

479 Lipids, proteins, and sites. J Cell Biol 204: 635-646.  
480  
481 Pollak NM, Schweiger M, Jaeger D, Kolb D, Kumari M, Schreiber R, Kolleritsch S,  
482 Markolin P, Grabner GF, Heier C, Zierler KA (2013) Cardiac-specific overexpression  
483 of perilipin 5 provokes severe cardiac steatosis via the formation of a lipolytic barrier.  
484 J Lipid Res 54: 1092-1102.  
485  
486 Sawada T, Miyoshi H, Shimada K, Suzuki A, Okamatsu-Ogura Y, Perfield II JW,  
487 Kondo T, Nagai S, Shimizu C, Yoshioka N, Greenberg AS. (2010) Perilipin  
488 overexpression in white adipose tissue induces a brown fat-like phenotype. PLoS  
489 ONE 5: e14006.  
490  
491 Shemesh Z, Leu S, Khozin-Goldberg I, Didi-Cohen S, Zarka A, Boussiba S (2016)  
492 Inducible expression of Haematococcus oil globule protein in the diatom  
493 Phaeodactylum tricornutum: Association with lipid droplets and enhancement of TAG  
494 accumulation under nitrogen starvation. Algal Res 18: 321-331.  
495  
496 Shi Q, Araie H, Bakku, RK, Fukao Y, Rakwal R, Suzuki I, Shiraiwa Y (2015) Proteomic  
497 analysis of lipid body from the alkenone-producing marine haptophyte alga  
498 *Tisochrysis lutea*. Proteomics 15: 4145-4158.  
499  
500 Sun Z, Miller RA, Patel RT, Chen J, Dhir R, Wang H, Zhang D, Graham MJ, Unterman  
501 TG, Shulman GI, Sztalryd C (2012) Hepatic Hdac3 promotes gluconeogenesis by  
502 repressing lipid synthesis and sequestration. Nat. Med. 18: 934-942.  
503

504 Sztalryd C, Kimmel AR (2014) Perilipins: Lipid droplet coat proteins adapted for  
505 tissue-specific energy storage and utilization, and lipid cytoprotection. *Biochimie* 96:  
506 96-101.

507

508 Vieler A, Brubaker SB, Vick B, Benning C (2012) A Lipid droplet protein on  
509 *Nannochloropsis* with functions partially analogous to plant oleosins. *Plant Physiol*  
510 158: 1562-1569.

511

512 Wang H, Sreenivasan U, Gong DW, O'Connell KA, Dabkowski ER, Hecker PA, Ionica  
513 N, Konig M, Mahurkar A, Sun Y, Stanley WC (2013) Cardiomyocyte-specific perilipin  
514 5 overexpression leads to myocardial steatosis and modest cardiac dysfunction. *J*  
515 *Lipid Res* 54: 953-965.

516

517 Yang L, Ding Y, Chen Y, Zhang S, Huo C, Wang Y, Yu J, Zhang P, Na H, Zhang H, Ma  
518 Y (2012) The proteomics of lipid droplets: structure, dynamics, and functions of  
519 organelle conserved from bacteria to humans. *J Lipid Res* 53: 1245-1253.

520

521 Yoneda K, Yoshida M, Suzuki I, Watanabe MM (2016) Identification of a major lipid  
522 droplet protein in a marine diatom *Phaeodactylum tricornutum*. *Plant Cell Physiol* 57:  
523 397-406.

524

525 Zaslavskaja LA, Lippmeier JC, Kroth PG, Grossman AR, Apt KE (2000)  
526 Transformation of the diatom *Phaeodactylum tricornutum* (Bacillariophyceae) with a  
527 variety of selectable marker and reporter genes. *J Phycol* 36: 379-386.

528

## Figure legends

Figure 1. Subcellular localization of StLDP–EGFP fusion protein.

Microscopic images of EGFP-expressing mutant (A) and StLDP–EGFP fusion protein-expressing mutant (B).

Figure 2. Growth curve, dry cell weight (DCW) and crude lipid amount, and expression levels of StLDP.

(A). Growth curve of wild type (WT) and StLDP-expressing mutant (H8). The cells were cultivated in the nitrogen-sufficient medium for 4 days, and then in the nitrogen-deficient medium for 6 days. Open circles indicate WT and open squares indicate H8 mutant. Values are shown as mean  $OD_{750} \pm SD$  ( $n = 3$ ). (B). DCW and crude lipid amount at the end of cultivation in WT and H8. (C). Relative expression of StLDP measured by real-time qRT-PCR. Expression levels were measured in samples on the initial day of reinoculation into the nitrogen-deficient medium (Day 4), and then after 3 and 6 days of cultivation in the nitrogen-deficient medium (Days 7 and 10, respectively). Expression levels in WT at Day 4 were considered as 1 (standard) and relative expression levels were calculated. Error bars indicate SD ( $n = 3$ ). Actin12 was used as a housekeeping gene for normalization.

Figure 3. Proportion of neutral and polar lipid in the crude lipid extract of WT and H8 mutant.

Neutral and polar lipid composition in WT and H8 mutant at Day 4 (A) and at Day 10 (B).

Error bars indicate SD, and statistical analyses were performed using Student's t-test

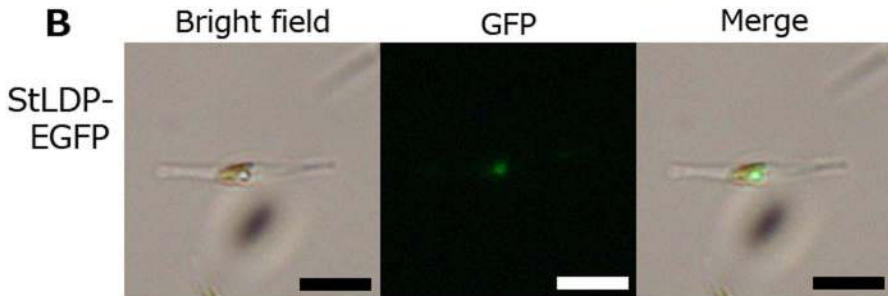
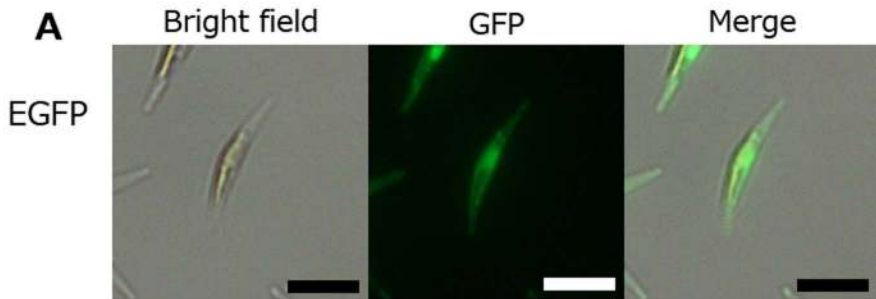
(\* $P < 0.05$ , \*\* $P < 0.01$ ,  $n = 3$ , one-tailed).

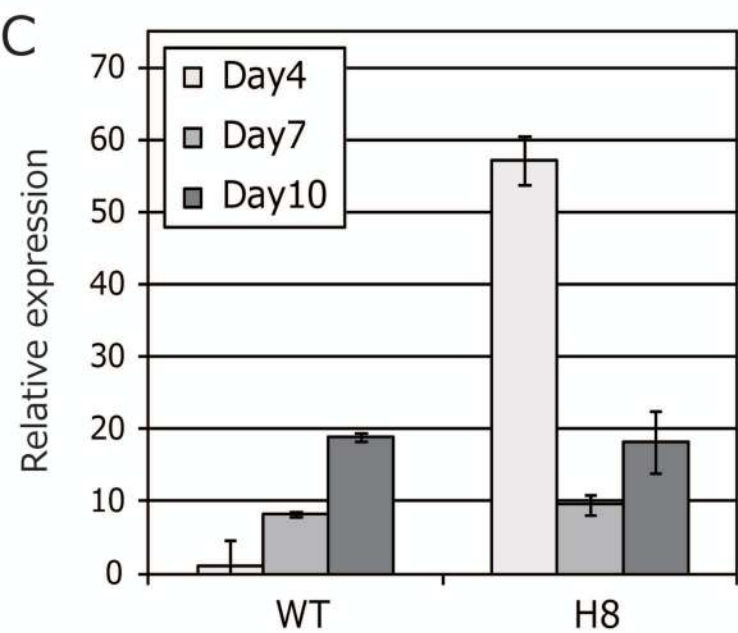
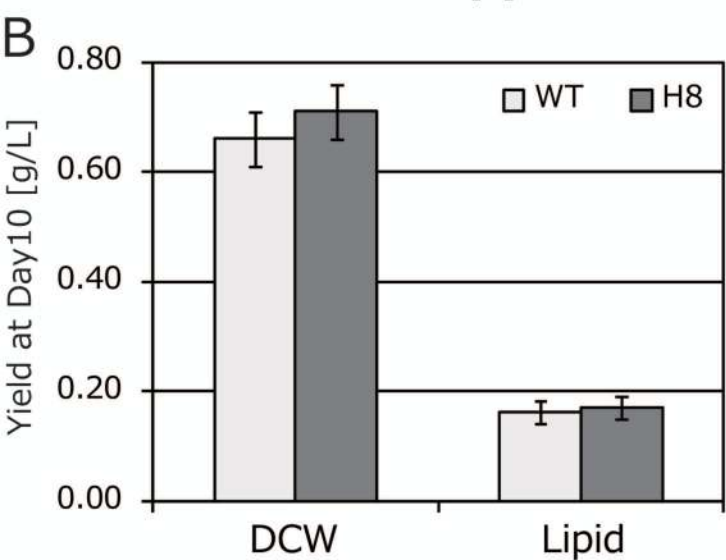
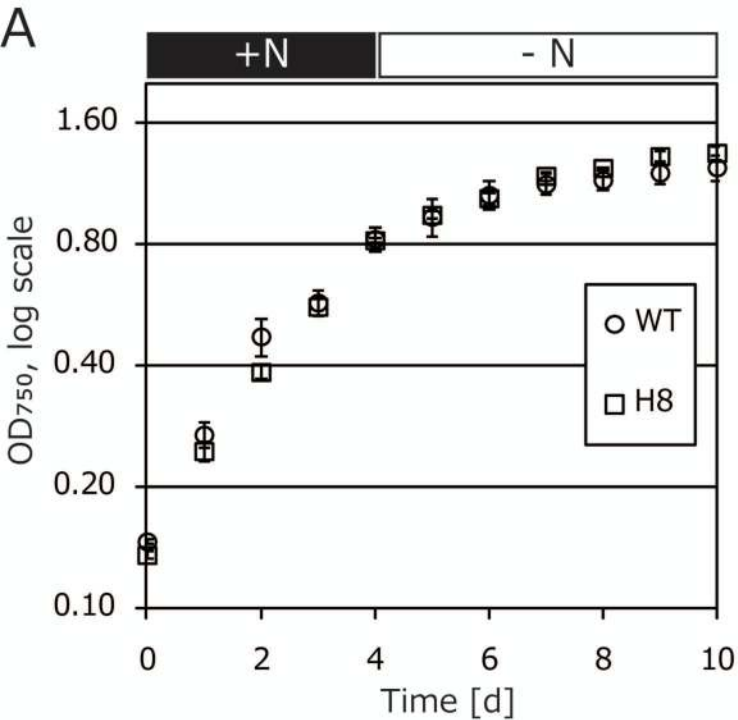
Figure 4. Microscopic images of lipid droplet formation in WT and H8 mutant. Nile-red stained cells at Day 4 (A), Day 6 (B), and at Day 10 (C). Fluorescent images were captured through a BNA green filter. Lipid droplets containing neutral lipid were visualized as green with the BNA filter. Scale bars represent 10  $\mu\text{m}$ .

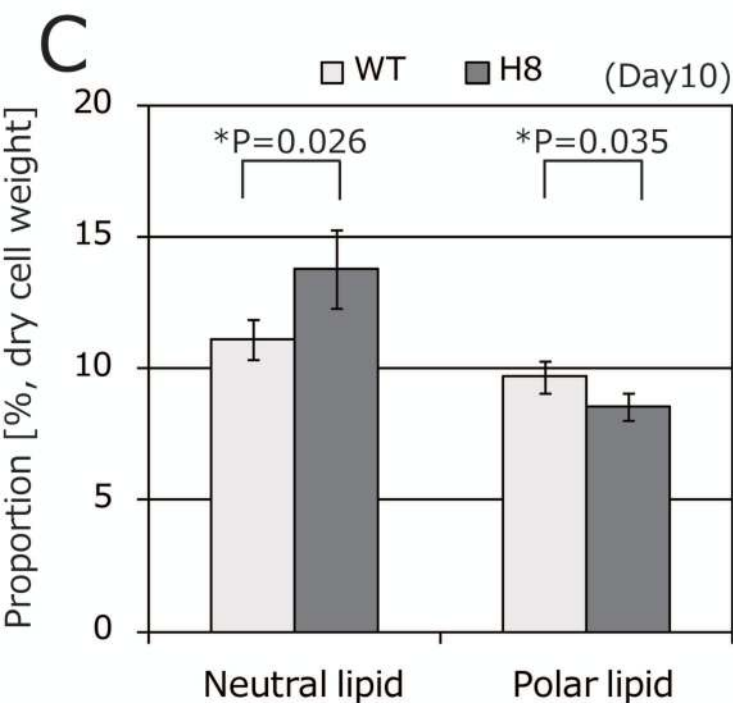
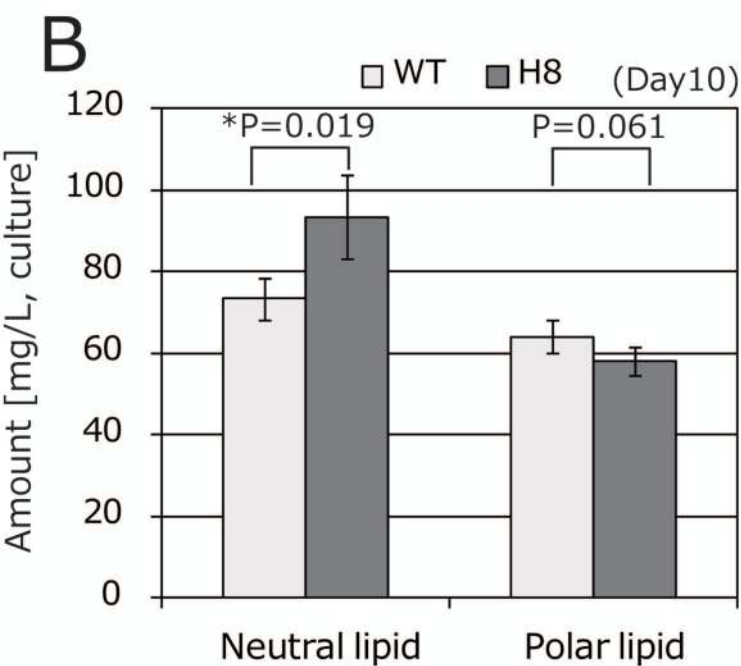
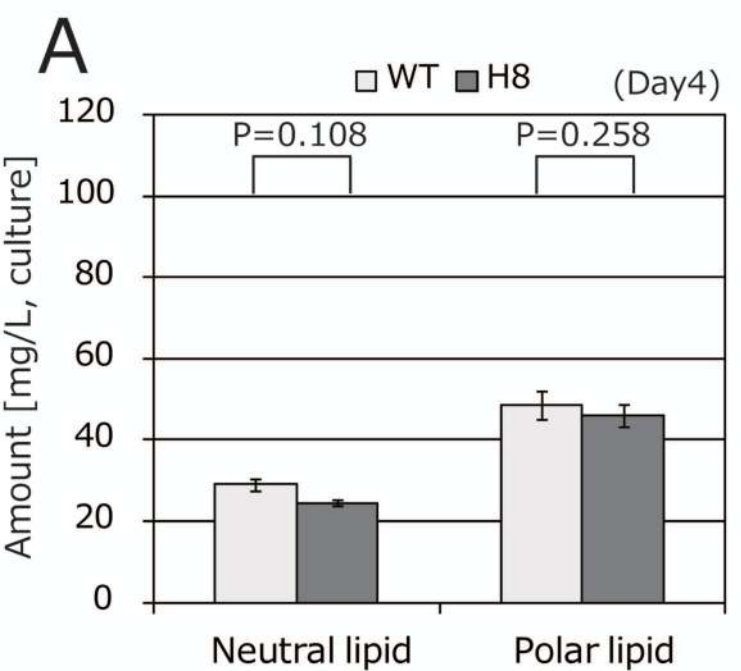
Figure 5. Distribution of the diameter of respective lipid droplets and the number of lipid droplets in single cells.

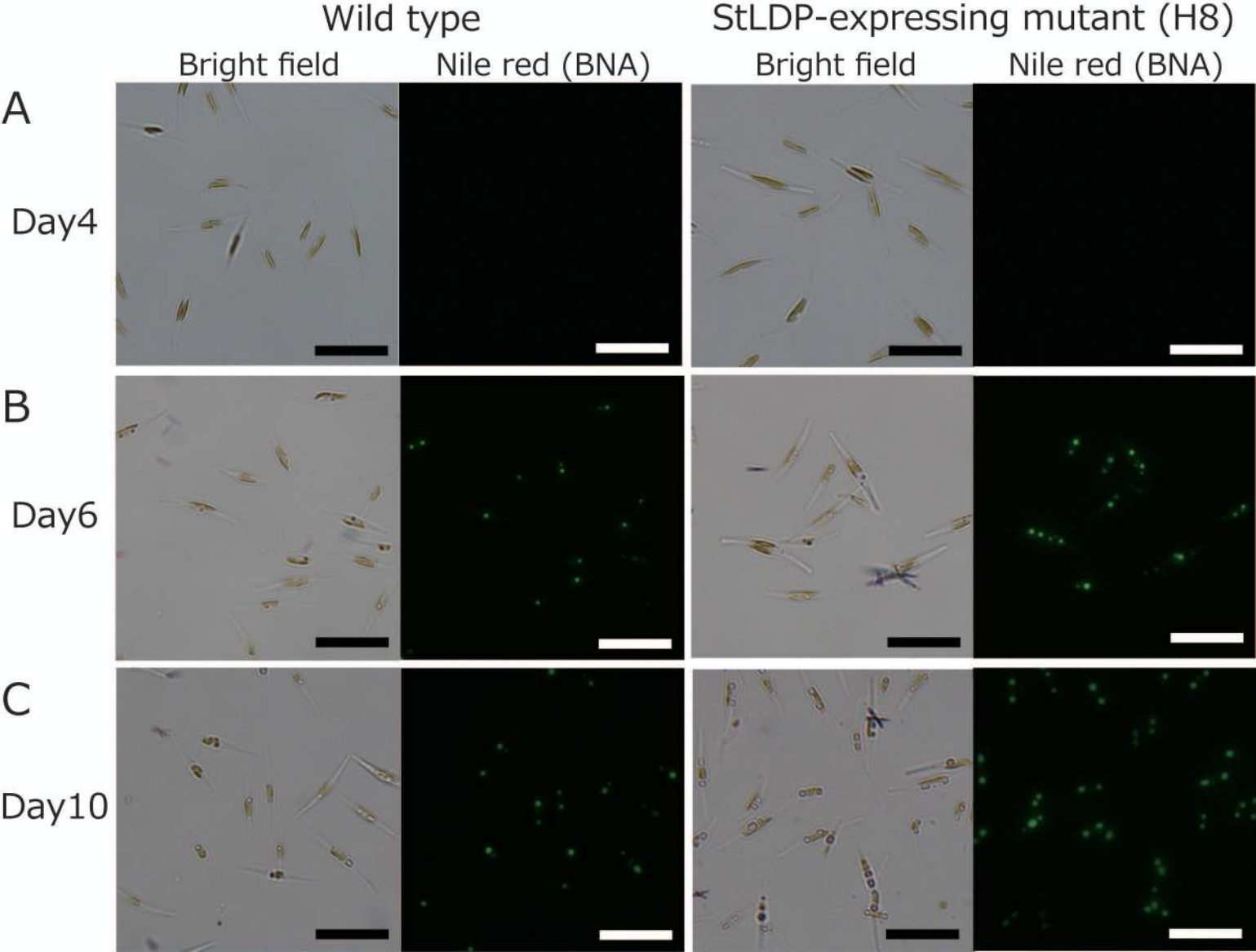
Size distribution of lipid droplets at Day 6 (A) (WT,  $n = 128$ ; H8,  $n = 151$ ) and at Day 10 (B) (WT,  $n = 268$ ; H8,  $n = 350$ ). Each droplet size was measured using ImageJ. (C). The number of lipid droplets per cell at Day 6 (WT,  $n = 99$ ; H8,  $n = 66$ ).

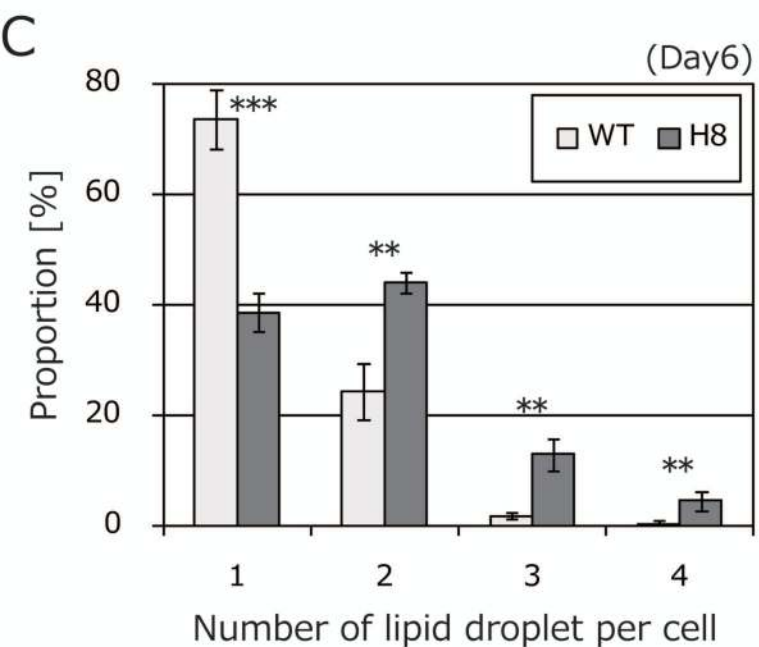
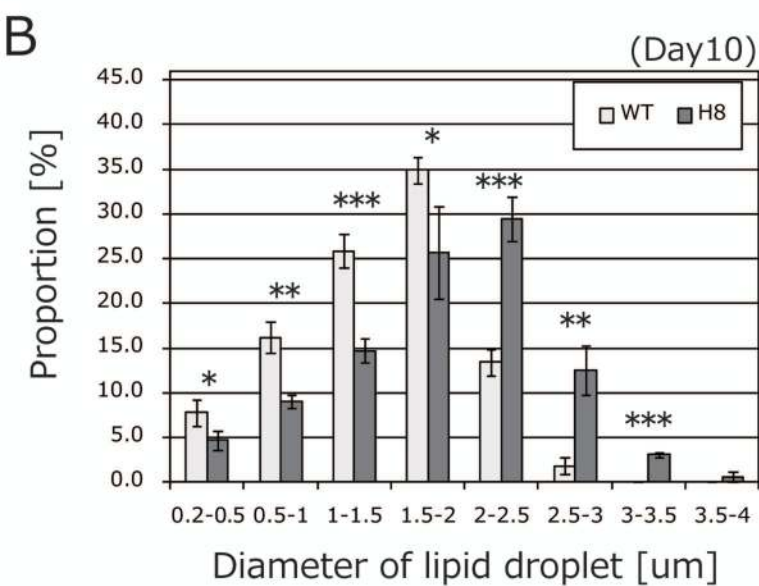
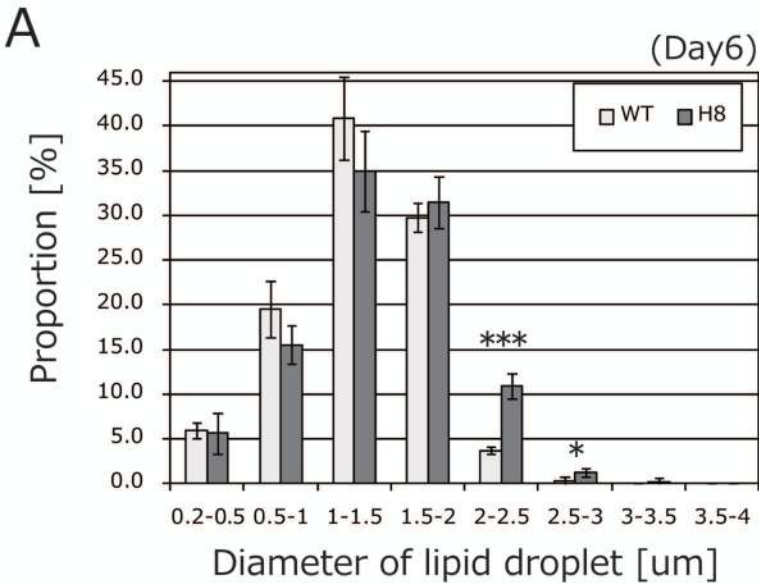












## Supplementary Data

Supplementary Table S1. Primers used in this study.

Primer name	Sequence
LD_F	5'-CGAGAATTCATGCCTTCTTCGAGCAATCC-3'
FP-LD_R	5'-CCTCGCCCTTGCTCACTCCACCTCCGCCTCCGCTTGCAGGAACA AGCAT-3'
FP-EGFP_F	5'-GCTTGTTCCCTGCAAGCGGAGGCGGAGGTGGAGTGAGCAAGGGC GAGGAG-3'
EGFP_R	5'-CTGAAGCTTTTACTTGTACAGCTCGTCCA-3'
LD-His_R	5'-CTGAAGCTTTTAGTGATGGTGGTGGTGGCTTGCAGGAACAA GCATGG-3'
6His-spe_R	5'-TTAGTGATGGTGGTGGTGGTGGTGG-3'